

# Isoconversional Analysis of Thermally Stimulated Effects in $\text{Cu}_x(\text{As}_2\text{Se}_3)_{100-x}$ Glasses

G.R. ŠTRBAC<sup>a</sup>, S. JARIĆ<sup>a,b</sup>, S.R. LUKIĆ-PETROVIĆ<sup>a</sup>,  
R. VIGI<sup>a</sup>, N. ČELIĆ<sup>a</sup> AND D.D. ŠTRBAC<sup>c</sup>

<sup>a</sup>University of Novi Sad, Faculty of Sciences, Department of Physics, Trg D. Obradovića 4, 21000 Novi Sad, Serbia

<sup>b</sup>University of Novi Sad, BioSense Institute, Dr Zorana Đinđića 1, 21000 Novi Sad, Serbia

<sup>c</sup>University of Novi Sad, Faculty of Technical Sciences, Trg D. Obradovića 6, 21000 Novi Sad, Serbia

Received: 29.11.2022 & Accepted: 06.03.2023

Doi: [10.12693/APhysPolA.143.369](https://doi.org/10.12693/APhysPolA.143.369)

\*e-mail: [grstrbac@uns.ac.rs](mailto:grstrbac@uns.ac.rs)

Through isoconversional analysis of differential scanning calorimetry data, thermally induced processes of glass transition and crystallization in  $\text{Cu}_x(\text{As}_2\text{Se}_3)_{100-x}$  chalcogenide glasses ( $x = 1, 5, 10$ , and  $15$  at.%) were investigated. The characteristic values of activation energy and its changes during the processes were calculated using the advanced isoconversional method developed by S. Vyazovkin as well as isoconversional forms of Kissinger and Moynihan relations. The results showed the variation of the activation energy with the extent of conversion. The activation energy values are slightly changing with the increase of Cu content from 1 to 5 at.%, while more significant changes are detected after a further increase of Cu content up to 15 at.%. The crystallization processes of  $\text{As}_2\text{Se}_3$  in composition with 1 at.% of Cu and  $\text{CuAsSe}_2$  and  $\text{Cu}_3\text{AsSe}_4$  in composition with 10 at.% of Cu were analyzed. Isoconversional analysis showed that crystallization is a complex process and that the apparent activation energy of crystallization of  $\text{As}_2\text{Se}_3$  and  $\text{CuAsSe}_2$  structural units decreases with the extent of conversion increase.

topics: glasses, thermal properties, thermal analysis, crystallization

## 1. Introduction

Chalcogenide glasses, especially those doped with certain elements (Ge, Cu, Ag, Sn, etc.), show very significant and unique chemical and physical properties, primarily electrical and optical, which, even today, make these materials attractive for scientific research and different applications [1–5]. Opportunities for the application of Cu-doped chalcogenide glasses are wide-ranging due to the possibility of programmed variations of the important thermal, thermo-mechanical, optical, structural, and electronic properties of chalcogenide glasses, induced by Cu introduction [6–11].

Glass transition and crystallization are very complicated processes whose nature has not been fully explained and is still the subject of current research in different classes of glass materials [12–18]. During the heating, glass alloys move from a region characterized by a slow change of the properties with the temperature to a glass transition region, in which changes in the properties are more dynamic and more significant. Due to the increase in temperature and rapid decrease in viscosity, cooperative movements of structural units are becoming more rapid, and the relaxation time of the structure decreases.

Further increase in temperature increases the mobility of structural elements, tending to transform into a crystalline structure characterized by a minimum of potential energy.

Characteristic temperature and activation energy are the two main parameters that characterize these processes. The kinetics of glass transition and crystallization processes is manifested through the dependence of characteristic temperature (glass transition temperature  $T_g$ , onset  $T_{onset}$ , or peak temperature  $T_p$  of the crystallization) on heating rate  $\beta$ . The apparent activation energy ( $E$ ) of such processes can be determined from this dependence. The dependence of  $E$  on the extent of conversion  $\alpha$  enables one to investigate the kinetics of the processes, indicating that these are multi-step processes. Knowledge of functional dependency  $E = E(\alpha)$  allows one to reliably predict the performance of a material.

Using the models of Kissinger [19, 20] and Moynihan/Mahadevan [21, 22] on different defined glass transition temperatures (in this paper, onset  $T_{go}$ , which represents the beginning of glass transition, and endset  $T_{ge}$ , which corresponds to the end of this process), changes in glass transition activation energy,  $E_g$ , throughout the process can be observed.

The isoconversional values of the activation energy can be calculated from the isoconversional rate dependence on temperature, without knowing the reaction model (“model-free” methods). Vyazovkin [23, 24] has developed the isoconversional method, which enables the determination of the apparent activation energy based on a series of measurements conducted at different heating rates. The value of  $E_\alpha$  can be determined at any specific value of the extent of conversion by a minimum of the objective function  $\Phi(E_\alpha)$ , defined as

$$\Phi(E_\alpha) = \sum_{i \neq j}^n \sum_j^n \frac{I(E_\alpha, T_{\alpha,i}) \beta_j}{I(E_\alpha, T_{\alpha,j}) \beta_i} = \min, \quad (1)$$

where  $n$  is the number of applied heating rates. In (1),  $I(E_\alpha, T_{\alpha,i})$  represents temperature integral

$$I(E, T) = \int_0^T dT \exp\left(-\frac{E}{RT}\right). \quad (2)$$

The activation energy changes during the glass transition/crystallization can also be determined by using the isoconversional forms (change of temperatures with the heating rate at constant  $\alpha$ ) of Kissinger [19, 20] and Moynihan/Mahadevan [21, 22] relations, respectively,

$$\frac{d \ln(\beta_i / T_{\alpha,i}^2)}{d(1/T_{\alpha,i})} = -\frac{E_\alpha}{R} \quad (3)$$

and

$$\frac{d \ln(\beta_i)}{d(1/T_{\alpha,i})} = -\frac{E_\alpha}{R}. \quad (4)$$

The objective of the research presented in this study is to investigate the changes in the apparent activation energy of glass transition and crystallization processes by applying isoconversional analysis and to provide a deeper insight into these processes, their nature, and the possibilities of controlling them. The aim is also to determine the influence of Cu content on investigated parameters and the correlation of kinetic parameters with structural changes, as well as to validate the results obtained by non-isoconversional and non-isothermal approaches [25].

## 2. Experiment

The investigated glasses of the  $\text{Cu}_x(\text{As}_2\text{Se}_3)_{100-x}$  composition, for  $x = 0, 1, 5, 10$ , and  $15$  at.%, were synthesized from elementary components (99.999% purity) by the cascade heating method [26]. The melts were air-quenched from the maximum temperature of synthesis. X-ray diffraction (XRD) and polarization microscopy methods were used for confirmation of the amorphous structure of the obtained samples.

In order to measure the caloric effects of the phase transformation and to study the glass transition and crystallization kinetics under non-isothermal

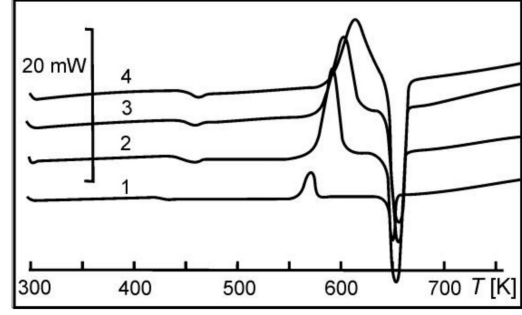


Fig. 1. DSC curves of the  $\text{Cu}_1(\text{As}_2\text{Se}_3)_{99}$  chalcogenide glass, at different heating rates: (1) 2 K/min, (2) 5 K/min, (3) 7.5 K/min, and (4) 10 K/min.

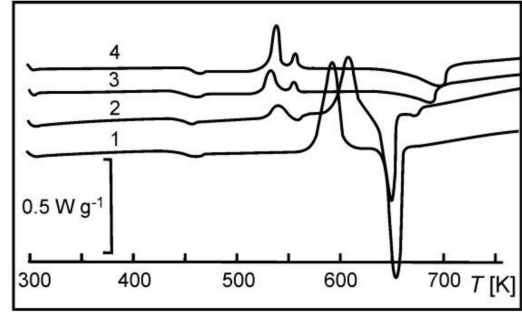


Fig. 2. DSC curves of chalcogenide glasses from the  $\text{Cu}_x(\text{As}_2\text{Se}_3)_{100-x}$  system: (1) 1 at.%, (2) 5 at.%, (3) 10 at.%, and (4) 15 at.% (at heating rate of 5 K/min).

conditions, Mettler Toledo DSC822<sup>e</sup> with a temperature accuracy of  $\pm 0.2$  K was used. Measurements were carried out from 300–773 K, with 50 ml/min of nitrogen flow. Bulk glass samples (weight  $\sim 15$  mg) sealed in the 40  $\mu\text{l}$  aluminum pans were thermally treated at different heating rates (2, 5, 7.5, 10, 20, and 30 K/min). The analysis of the glass transition and crystallization, deconvolution of a complex peak, and determination of the characteristic temperatures were done using the supporting STAR Software.

XRD measurements were conducted on Rigaku MiniFlex 600 instrument in an angle interval of  $20$ – $90^\circ$ .

## 3. Results and discussion

The differential scanning calorimetry (DSC) curves of the  $\text{Cu}_1(\text{As}_2\text{Se}_3)_{99}$  chalcogenide glass, recorded at different heating rates, are presented in Fig. 1 as an example.

Figure 2 shows DSC curves for all the investigated compositions from the  $\text{Cu}_x(\text{As}_2\text{Se}_3)_{100-x}$  system, obtained at a heating rate of 5 K/min, confirming that they are markedly dependent on the glass composition.

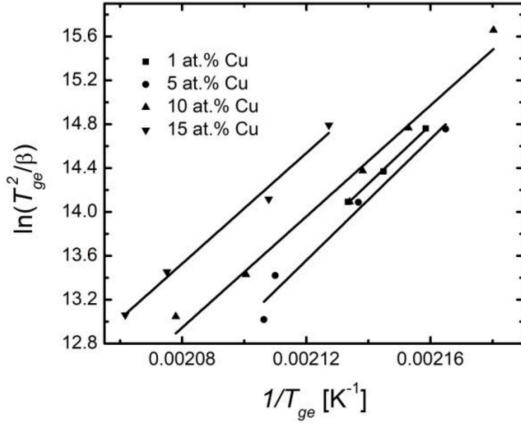


Fig. 3. Dependence of  $\ln(T_{ge}^2/\beta_i)$  on  $1/T_{ge}$  of the investigated  $\text{Cu}_x(\text{As}_2\text{Se}_3)_{100-x}$  glasses.

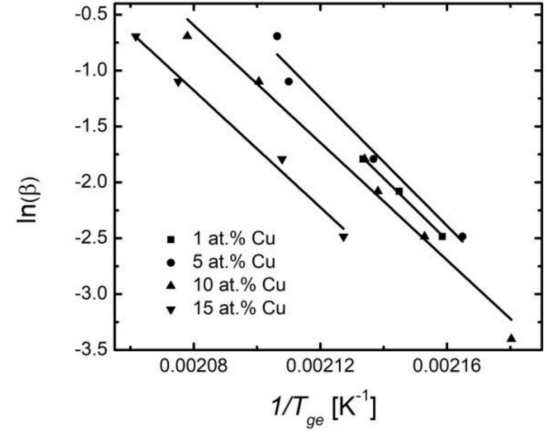


Fig. 4. Dependence of  $\ln(\beta_i)$  on  $1/T_{ge}$  of the investigated  $\text{Cu}_x(\text{As}_2\text{Se}_3)_{100-x}$  glasses.

TABLE I

Values of apparent activation energy calculated for onset [27] and endset glass transition temperatures according to Kissinger and Moynihan models.

$x$ [at.%]	Kissinger [kJ/mol]		Moynihan [kJ/mol]	
	$E_{go}$ [27]	$E_{ge}$	$E_{go}$ [27]	$E_{ge}$
1	266(21)	223(11)	273(21)	231(11)
5	311(15)	230(28)	318(15)	238(28)
10	319(36)	211(16)	327(36)	218(16)
15	288(10)	210(16)	296(10)	217(16)

As can be seen in Figs. 1 and 2, three effects occurred throughout the applied heating treatment of glasses from the investigated system. An endothermic effect which occurs at about 450 K, corresponds to the glass transition process.

### 3.1. Glass transition

In order to assess if there is a change in apparent activation energy during the glass transition process, by using the standard relations of Moynihan and Kissinger for endset glass transition temperature,  $T_{ge}$  (the end of the process), values of this parameter were determined, and results were compared with results obtained for onset glass transition temperature,  $T_{go}$  (the beginning of the process) [27]. Figures 3 and 4 present the dependence of  $\ln(T_{ge}^2/\beta_i)$  and  $\ln(\beta_i)$  on  $1/T_{ge}$  for all investigated samples. The values of apparent activation energies  $E_{ge}$  are presented in Table I.

For any of the investigated glass compositions, there is a decrease in the value of activation energy  $E_g$  throughout the glass transition process, pointing out that this is not a single-step process. Values of  $E_{ge}$  indicate that for compositions with 1 and 5 at.% of Cu, there are no significant changes in this parameter, while compositions with 10 and 15 at.% Cu have slightly lower values. It should be noted that

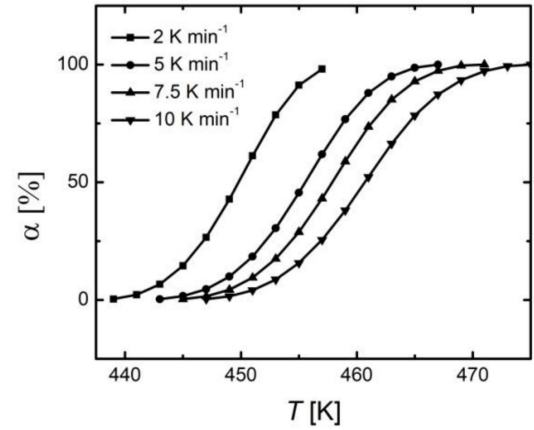


Fig. 5. Extent of conversion dependence on temperature of the  $\text{Cu}_1(\text{As}_2\text{Se}_3)_{99}$  glass at different heating rates.

the  $E_{go}$  exhibits somewhat different behavior [27], but the values of this parameter were determined with significant uncertainty, so the effect of Cu introduction on the  $E_{go}$  could not be accurately analyzed.

The isoconversional Vyazovkin model (with the Gorbachev approximation) was used for further analysis of the variation in the  $E_g$  and a better understanding of the glass transition process. Isoconversional analysis was also performed by using the isoconversional forms of the Kissinger and Moynihan equations (see (3) and (4)). Isoconversional methods can be applied to the DSC data on a glass transition after the determination of an extent of conversion,  $\alpha$ . As DSC measures a change in heat during the process,  $\alpha$  is evaluated as a ratio of the current heat change to the total heat of the whole process. The obtained results indicated that the process of glass transition occurs in parallel with the effect of overheating. The dependence of the extent of conversion on temperature for  $\text{Cu}_1(\text{As}_2\text{Se}_3)_{99}$  glass at different heating rates

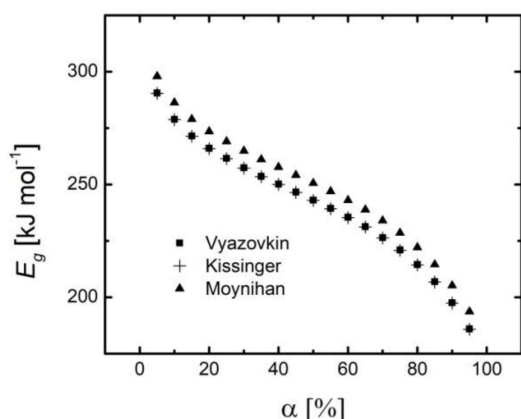


Fig. 6. Apparent glass transition activation energy  $E_g$  dependence on extent of conversion of the  $\text{Cu}_1(\text{As}_2\text{Se}_3)_{99}$  glass.

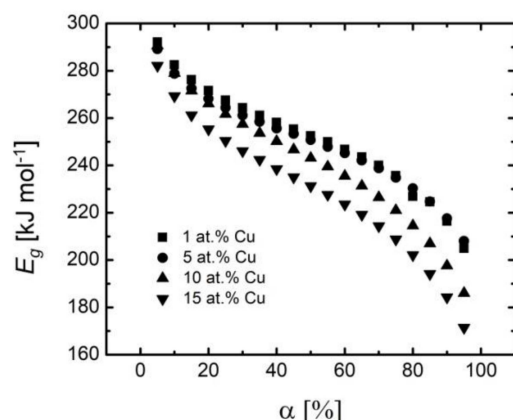


Fig. 7. Apparent glass transition activation energy  $E_g$  dependence on extent of conversion of the  $\text{Cu}_x(\text{As}_2\text{Se}_3)_{100-x}$  glasses.

are presented in Fig. 5. The results of the application of the isoconversional models to this particular glass are presented in Fig. 6.

The results evidently show a decrease in the activation energy of the glass transition, indicating that it is a complex process. The value of  $E_g$  decreased from 292(13) to 205(16) kJ/mol in the composition with 1 at.% of Cu. This decrease is a consequence of the increase in the available volume during heating, which enables freer cooperative movements of structural units. Activation energy values themselves (of the order of several hundred kJ) indicate cooperative movements. Generally, structural units of the glass matrix can move cooperatively or freely in a non-cooperative manner. While glass relaxes towards the equilibrium supercooled liquid structure, both cooperative and non-cooperative motions take place during the process. These two kinds of motion have markedly different dependencies of the relaxation time on temperature, and the kinetics of relaxation is dominated by the fastest process. Also, it can be observed that the values obtained by apply-

ing the Kissinger and Vyazovkin models are almost the same as those reported for other chalcogenide systems [27–30]. The activation energy changes during the glass transition process for samples with different Cu content are shown in Fig. 7.

Comparison with the results from the classical analysis showed a very good agreement. Compositions with 1 and 5 at.% of Cu are characterized by almost the same values of  $E_g$ . Glasses with 10 and 15 at.% Cu have slightly lower values of  $E_g$ . The decrease in activation energy with increasing Cu content indicates greater thermodynamic stability and easier movements of structural units in the compound. Cu introduction causes changes in the kinetic parameters of the amorphous matrix. The change in the trend of the apparent activation energy dependence on the Cu content in the glass composition can be explained by the dominant formation of the structural units in which Cu coordination is higher. The situation becomes more complex due to the fact that Cu, by forming units with As and Se, binds more Se, thus shifting the glass matrix to the area which is richer in As (from ratio 2:3), yielding the formation of new structural units, probably  $\text{As}_4\text{Se}_4$ .  $\text{As}_4\text{Se}_4$  molecular species can exist as ethylene-like polymerized units in addition to forming cage-like molecules [31]. Also, the formation of the  $\text{As}_4\text{Se}_3$  units may be expected.

### 3.2. Crystallization

The exothermic effect of crystallization of individual structural units in the glass after the glass transition peak can be observed (temperature from 520–615 K). Sample with 1 at.% of Cu exhibits only one crystallization and one melting peak, and, as already discussed, those processes correspond to the  $\text{As}_2\text{Se}_3$  structural unit [25]. In the  $\text{Cu}_5(\text{As}_2\text{Se}_3)_{95}$  and  $\text{Cu}_{10}(\text{As}_2\text{Se}_3)_{90}$  glasses, crystallization of  $\text{As}_2\text{Se}_3$  also takes place, the share of which rapidly declines with the increase of the applied heating rate. The increase of Cu content in investigated glass alloys triggers the crystallization of two other structural units, i.e.,  $\text{CuAsSe}_2$  (at a lower temperature of crystallization) and  $\text{Cu}_3\text{AsSe}_4$ . Endothermic effects corresponding to the melting of  $\text{CuAsSe}_2$  crystal units occur with the further increase in temperature.

The ternary system Cu–As–Se is a complex system in which a long list of candidates for possible crystallizing species can be expected, as indicated by the detailed analysis of phase equilibrium in this system [32] and the phase diagram of the  $\text{Cu}_2\text{Se}-\text{As}_2\text{Se}_3$  system [33].

In order to determine the phases present, samples, annealed according to results from DSC measurements at three temperatures (555, 620, and 750 K), were characterized by using XRD. Figure 8 shows the XRD peaks of the annealed  $\text{Cu}_{15}(\text{As}_2\text{Se}_3)_{85}$  glass sample. In this case, identification is significantly more difficult since both units,

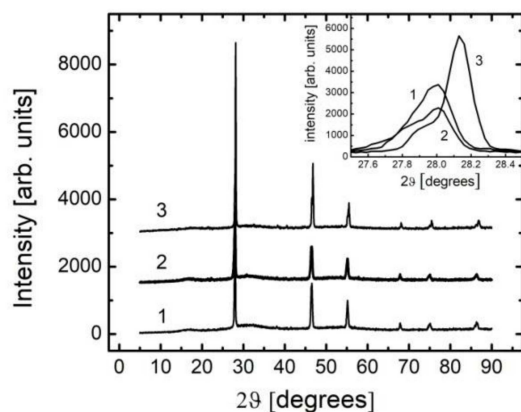


Fig. 8. XRD pattern of  $\text{Cu}_{15}(\text{As}_2\text{Se}_3)_{85}$  glass after annealing at (1) 555 K, (2) 620 K, and (3) 750 K.

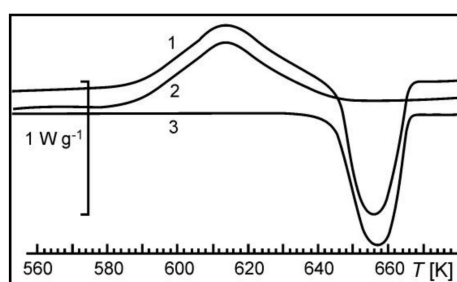


Fig. 9. Deconvolution of crystallization and melting peak of the  $\text{As}_2\text{Se}_3$  structural unit in the  $\text{Cu}_1(\text{As}_2\text{Se}_3)_{99}$  glass at heating rate of 10 K/min: (1) original DSC curve, (2) peak of crystallization, (3) melting peak.

$\text{CuAsSe}_2$  and  $\text{Cu}_3\text{AsSe}_4$ , have a crystal structure close to sphalerite, and their diffraction patterns are very similar. Due to small distortions from the sphalerite structure, peak splitting into doublets occurs. This is somewhat more pronounced with the  $\text{Cu}_3\text{AsSe}_4$  unit [34]. The complex shape of the peaks and the small change in the position of the maximum at different temperatures (inserted figure in Fig. 8) indicate that it is still a diffractogram of a mixture of two units, i.e., these peaks are a consequence of overlapping peaks of individual components. The maxima of the  $\text{CuAsSe}_2$  structural unit are at slightly lower angle values. A slight shift in the position of the maximum at higher heating temperatures indicates that then the  $\text{Cu}_3\text{AsSe}_4$  structural unit dominates.

The performed XRD analysis clearly showed that the structural units are  $\text{CuAsSe}_2$  and  $\text{Cu}_3\text{AsSe}_4$ , and therefore that the second exothermic peak from the DSC measurements does not correspond to the  $\text{Cu}_2\text{Se}$  unit, as previously stated in [25] without direct experimental confirmation. The crystallization kinetic parameters determined in [25] actually describe and correspond to the crystallization of the  $\text{Cu}_3\text{AsSe}_4$  structural unit.

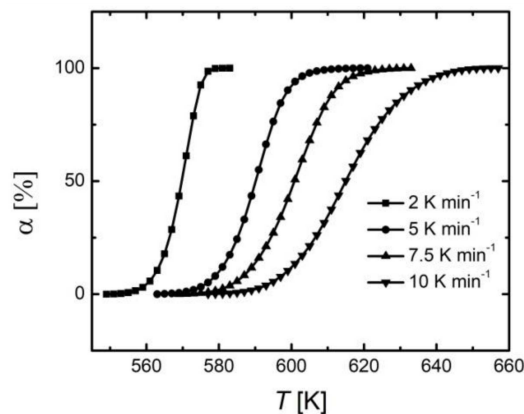


Fig. 10. Extent of crystallization conversion of the  $\text{As}_2\text{Se}_3$  structural unit as a function of temperature in the  $\text{Cu}_1(\text{As}_2\text{Se}_3)_{99}$  glass.

The introduction of Cu enables crystallization of the  $\text{As}_2\text{Se}_3$  structural unit at lower temperatures in comparison with composition without Cu, where mechanically induced defects and a number of stress-induced defects are crystallization centers [25]. In glass alloy with 1 at.% of Cu, the crystallization peak is partially overlapped by melting at a heating rate of 10 K/min, so a deconvolution of peaks was performed (Fig. 9).

The crystallization processes of  $\text{CuAsSe}_2$  and  $\text{Cu}_3\text{AsSe}_4$  structural units are also overlapped, so for the purpose of analysis, deconvolution of these peaks was done. A peak separation on obtained curves, up to the degree that enables the identification of peak shape, is needed because the crystallization peaks do not have mathematically defined functional dependence. The peak shape depends on the mechanism of nucleation and crystal growth. Isoconversional analysis was performed on these units only for  $\text{Cu}_{10}(\text{As}_2\text{Se}_3)_{90}$  by using the isoconversional form of Kissinger (see (3)) and Moynihan (see (4)) equations, as well as the Vyazovkin model (see (1)) with the Gorbachev approximation). Figure 10 shows the dependence of the extent of conversion on temperature for  $\text{As}_2\text{Se}_3$  in the composition with 1 at.% of Cu as an example.

The results of these analyses, which show the dependence of apparent activation energy of crystallization,  $E_c$ , on the extent of conversion, are shown in Figs. 11–13. The obtained data clearly show a change in the activation energy  $E_c$ , indicating that crystallization is also a complex process. The obtained values are in good correlation with the values obtained by using non-isothermal and non-isoconversion models [25].

Processes such as molecular rearrangements, which include rotation, bending, and breaking of existing bonds, take place during crystal growth. Considering that the activation energy quantifies the ease of molecular rearrangement, it can be



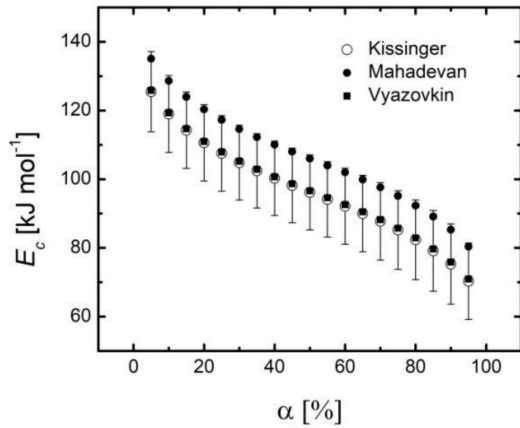


Fig. 11. Apparent activation energy of crystallization  $E_c$  of the  $\text{As}_2\text{Se}_3$  structural unit as a function of extent of conversion in the  $\text{Cu}_1(\text{As}_2\text{Se}_3)_{99}$  glass.

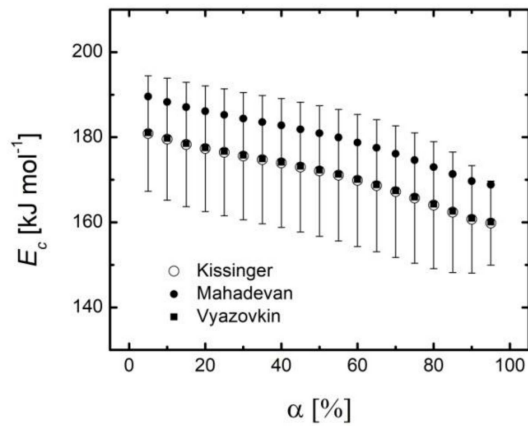


Fig. 12. Apparent activation energy of crystallization  $E_c$  of the  $\text{CuAsSe}_2$  structural unit as a function of extent of conversion in the  $\text{Cu}_{10}(\text{As}_2\text{Se}_3)_{90}$  glass.

concluded that in the investigated glasses, these processes most easily occurred in the case of  $\text{As}_2\text{Se}_3$  structural units, with  $E_c$  of 96(11) kJ/mol for  $\alpha = 0.5$ . Earlier analysis [25] indicates that crystallization takes place via volume nucleation and three-dimensional growth with a variable number of nucleation centers. Centers of nucleation are formed during the crystallization process. Values of  $E_c$  for structural units  $\text{CuAsSe}_2$  and  $\text{Cu}_3\text{AsSe}_4$  at the same value of  $\alpha$  were 172(15) and 281(12) kJ/mol, respectively. The crystallizations of  $\text{CuAsSe}_2$  and  $\text{Cu}_3\text{AsSe}_4$  are shifted to the lower temperature region.

According to previous investigations [25],  $\text{Cu}_{10}(\text{As}_2\text{Se}_3)_{90}$  glass alloy contained a sufficiently large number of nucleation centers before the experiment, and their number did not increase significantly during the crystal growth. Crystallization is characterized by volume nucleation with a constant number of nuclei. The activation energy refers mostly to crystal growth.

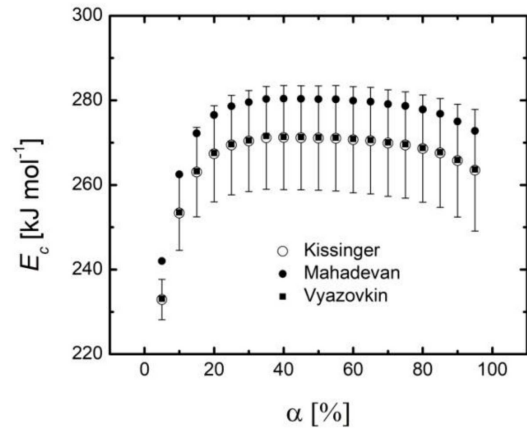


Fig. 13. Apparent activation energy of crystallization  $E_c$  of the  $\text{Cu}_3\text{AsSe}_4$  structural unit as a function of extent of conversion in the  $\text{Cu}_{10}(\text{As}_2\text{Se}_3)_{90}$  glass.

Isoconversional analysis showed that the apparent activation energy of crystallization of  $\text{As}_2\text{Se}_3$  and  $\text{CuAsSe}_2$  structural units decreases with an increase in the extent of transformation. For the  $\text{Cu}_3\text{AsSe}_4$  structural unit, the apparent activation energy initially increases for small values of the extent of transformation and then shows a slight decreasing tendency. This indicates that the crystallization of  $\text{Cu}_3\text{AsSe}_4$  was initially hindered by the incomplete crystallization of the  $\text{CuAsSe}_2$  structural unit.

#### 4. Conclusions

Isoconversional analysis was used to analyze thermally induced processes of glass transition and crystallization in glass alloys from the  $\text{Cu}_x(\text{As}_2\text{Se}_3)_{100-x}$  system for  $x = 0, 1, 5, 10$ , and 15 at.%. By applying the Kissinger and Moynihan models to the onset and endset glass transition temperature, variation of  $E_g$  with temperature was observed. This variation of  $E_g$  was additionally studied using the Vyazovkin isoconversional model as well as isoconversional forms of Kissinger and Moynihan equations, and previously noticed non-linear decrease was attributed to a complex process. The values of the activation energy indicate that the structural units move cooperatively, and their motion becomes easier with the extent of conversion increase. The decrease in activation energy with increasing Cu content, from about 250 kJ/mol at the extent of conversion of 50 % for 1 and 5 at.% of Cu content to 231 kJ/mol for composition with 15 at.% at the same values of the extent of conversion, indicates greater thermodynamic stability. The obtained results refer that Cu is actively incorporated into the glass matrix by forming units with selenium and arsenic (binding more Se), causing changes in the glass structure.

Isoconversional analysis of the crystallizations of  $\text{As}_2\text{Se}_3$ ,  $\text{CuAsSe}_2$ , and  $\text{Cu}_3\text{AsSe}_4$  was done, showing that these are complex processes with apparent activation energies of 96(11), 172(15), and 271(12) kJ/mol, respectively, at  $\alpha = 0.5$ . Crystallization is easiest to perform in the case of  $\text{As}_2\text{Se}_3$ . Unlike  $\text{As}_2\text{Se}_3$  and  $\text{CuAsSe}_2$ , in the case of the  $\text{Cu}_3\text{AsSe}_4$  structural unit, the activation energy during the crystallization initially increased and then slightly decreased as a result of the unfinished crystallization of  $\text{CuAsSe}_2$ .

### Acknowledgments

The authors acknowledge the financial support of the Provincial Secretariat for Higher Education and Scientific Research (Project: Novel chalcogenide materials for efficient transformation and use of energy, No.142-451-3128/2022-01/2) and the Ministry of Education, Science and Technological Development of the Republic of Serbia (Grant No. 451-03-68/2022-14/200125).

### References

- [1] A.I. Lacaita, *Solid State Electron.* **50**, 24 (2006).
- [2] R. Kaplan, B. Kaplan, *Acta Phys. Pol. A* **135**, 332 (2019).
- [3] H. Kim, W.H. Lee, J.H. Lee, D.K. Kwon, Y.S. Song, Y.G. Choi, *Ceram. Int.* **45**, 12010 (2019).
- [4] T.V. Moreno, L.C. Malacarne, M.L. Baesso, W. Qu, E. Dy, Z. Xie, J. Fahlman, J. Shen, N.G.C. Astrath, *J. Non-Cryst. Solids* **495**, 8 (2018).
- [5] M.V. Šiljegović, S.R. Lukić-Petrović, D.M. Petrović, I.R. Videnović, I.I. Turyanytsa, *Acta Phys. Pol. A* **129**, 488 (2016).
- [6] A.A. Soliman, *Thermochim. Acta* **423**, 71 (2004).
- [7] P. Priyadarshini, S. Das, R. Naik, *RSC Adv.* **12** 9599 (2022).
- [8] D.M. Guzman, A. Strachan, *Phys. Rev. Mater.* **1**, 055801 (2017).
- [9] T.S. Kavetsky, V.F. Valeev, V.I. Nuzhdin, V.M. Tsmots, A.L. Stepanov, *Tech. Phys. Lett.* **39**, 1 (2013).
- [10] S.R. Lukić, D.M. Petrović, D.D. Štrbac, V.B. Petrović, F. Skuban, *J. Therm. Anal. Calorim.* **82**, 41 (2005).
- [11] K. Ogusu, K. Shinkawa, *Opt. Exp.* **17**, 8165 (2009).
- [12] R. Svoboda, *J. Non-Cryst. Solids* **510**, 6 (2019).
- [13] P. Gong, F. Li, G. Yin, L. Deng, X. Wang, J. Jin, *J. Therm. Anal. Calorim.* **142**, 63 (2020).
- [14] R. Svoboda, D. Brandova, *J. Alloy. Compd.* **770**, 564 (2019).
- [15] M.M. Rahvard, M. Tamizifar, S.M.A. Boutorabi, *J. Therm. Anal. Calorim.* **134**, 903 (2018).
- [16] S. Saini, A.P. Srivastava, S. Neogy, *J. Alloy. Compd.* **772**, 961 (2019).
- [17] K.H. Lee, Q. Zheng, J. Ren, C.J. Wilkinson, Y. Yang, K. Doss, J.C. Mauro, *J. Non-Cryst. Solids* **521**, 119534 (2019).
- [18] R. Raonić, N.M. Čelić, S.R. Lukić-Petrović, G.R. Štrbac, *Acta Phys. Pol. A* **140**, 235 (2021).
- [19] H.E. Kissinger, *Anal. Chem.* **29**, 1702 (1957).
- [20] H.E. Kissinger, *J. Res. Natl. Bur. Stand.* **57**, 217 (1956).
- [21] C.T. Moynihan, P.B. Macedo, *J. Phys. Chem.* **78**, 2673 (1974).
- [22] S. Mahadevan, A. Giridhar, A.K. Singh, *J. Non-Cryst. Solids* **88**, 11 (1986).
- [23] S. Vyazovkin, *J. Comput. Chem.* **22**, 178 (2001).
- [24] S. Vyazovkin, D. Dollimore, *Chem. Inf. Comput. Sci.* **36**, 42 (1996).
- [25] G.R. Štrbac, D.D. Štrbac, S.R. Lukić-Petrović, M.V. Šiljegović, *J. Non-Cryst. Solids* **426**, 92 (2015).
- [26] D.M. Petrović, S.R. Lukić, A.F. Petrović, F. Skuban, in: *Abstracts Book E-MRS Fall Conference*, Strasbourg, France 1990, p. 106.
- [27] G. Štrbac, S. Lukić-Petrović, D. Štrbac, K. Čajko, I.I. Turyanytsa, *Acta Phys. Pol. A* **123**, 256 (2013).
- [28] A.H. Moharram, M.A. El-Oyoun, *Appl. Phys. A* **116**, 311 (2014).
- [29] A.A. Elabbar, *J. Alloy. Compd.* **476**, 125 (2009).
- [30] A.S. Soltan, A.A. Abu-Sehly, A.A. Joraid, S.N. Alamri, *Thermochim. Acta* **574**, 73 (2013).
- [31] M. Mitkova, P. Boolchand, *J. Non-Cryst. Solids* **240**, 1 (1998).
- [32] K. Cohen, J. Rivet, J. Dugue, *J. Alloy. Compd.* **224**, 316 (1995).
- [33] R. Blachnik, G. Kurz, *J. Solid State Chem.* **55**, 218 (1984).
- [34] K.S. Liang, A. Bienenstock, C.W. Bates, *Phys. Rev. B* **10**, 1528 (1974).